ISBN: 978-3-95450-191-5 doi:10.18429/JACoW-SRF2017-THXA03

CRAB CAVITIES FOR THE HIGH-LUMINOSITY LHC*

Rama Calaga, CERN, Geneva, Switzerland

Abstract

As a first step towards the realization of crab crossing for High-Luminosity LHC (HL-LHC), two superconducting crab cavities are foreseen to be tested for the first time in the SPS with protons. The progress on the cavity fabrication, RF test results, cryomodule development and integration into the SPS are presented. Some aspects of the beam tests with crab cavities in the SPS are outlined.

INTRODUCTION

A luminosity upgrade of the LHC is planned for 2024-25 to extend the lifetime and physics reach of the LHC into the next decade. This upgrade will increase the integrated luminosity potential by ten-fold to 300 fb^{-1}/yr from the present LHC [1]. Two key superconducting technologies are required to enable this upgrade high field large aperture quadrupoles and high field compact crab cavities. Fig 1 shows a schematic layout of the interaction region upgrade (to to scale).

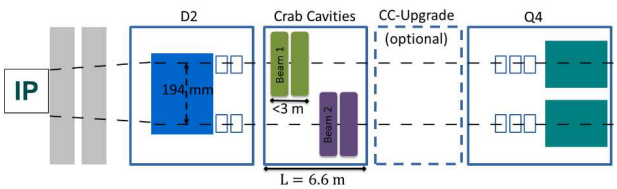

Figure 1: Schematic of the LHC interaction region and the respective magnetic and RF elements to be upgraded for HL-LHC.

Some relevant parameters for the LHC design and upgrade are listed in Table 2.

Table 1: Some relevant parameters for the LHC nominal and upgrade lattices.

	Unit	LHC	HL-LHC
Energy	[TeV]	7	7
p/bunch	[10^{11}]	1.15	2.2
Bunch Spacing	[ns]	25	25
ϵ_n (x,y)	[µm]	2.5	2.5
σ_z (rms)	[cm]	7.55	9.0
$IP_{1,5}$ β^*	[cm]	55	20
Betatron Tunes	-	64.31, 59.32	62.31, 60.32
X-Angle: $2\phi_c$	[µrad]	300	590
Piwinski Angle	$\frac{\sigma_z}{\sigma^*}\phi_c$	0.65	3.14
RF Frequency	[MHz]	400.79	
Peak luminosity	[10^{34}cm^{-2}s^{-1}]	1.0	7.2

* Research supported by the HL-LHC project and the DOE, UK-STFC and KEK

CRAB CAVITIES

Without crab crossing in the HL-LHC, the beams see each other at more than 128 locations excluding the collision points due to the fact that they share a common beam pipe in the four interaction regions. Separation between the counter rotating beams is accomplished by introducing a crossing angle at the interaction point (IP), which needs to increase with the inverse of the transverse beam size to maintain a constant normalized beam separation.

The non-zero crossing angle implies an inefficient overlap of the colliding bunches. The luminosity reduction compared to that of a zero crossing angle, assuming a Gaussian distribution, can be conveniently expressed by a reduction factor,

$$R_\Phi = \frac{1}{\sqrt{(1+\Phi^2)}} \quad (1)$$

where $\Phi = \sigma_z\phi/\sigma_x$ is the Piwinski angle, σ_z is the bunch length, σ_x is the beam size and ϕ is the half crossing angle at the IP. As shown in Table 2, a Piwinski angle as large as 3 results in a the peak luminosity loss of more than 70%.

Therefore, to fully exploit the available luminosity, a time-dependent transverse kick from an RF deflecting cavity applied. This action rotates the bunch in the $x-z$ (or $y-z$) plane about the barycentre of the bunch (see Fig. 2). The kick is transformed to a relative displacement of the head and the tail of the bunch at the IP after a phase advance of 90° to impose a head-on collision. The advantage of this technique is that the required beam separation to minimize parasitic collisions is still maintained without loss of luminosity. This effect can also be viewed as z-dependent dispersive orbit. The upstream RF deflector is used to reverse the kick to confine the bunch rotation to within the IR.

Figure 2: Schematic of the bunch crossings at the IP with and without crab cavities.

Since the crossing plane in the two high luminosity experiments is different, a local crab cavity system is a prerequisite. The required HL-LHC crossing angle together with the beam optics require the crab cavities to provide a total voltage of 12 – 13 MV per beam per side of each collision point at a frequency of 400.79 MHz. The present baseline for HL-LHC will use a two-cavity cryomodule as the basic unit on each side of the IP per beam. Each cryomodule will provide a total deflecting voltage of 6.8 MV (3.4 MV per cavity). The additional voltage required for the full compensation is kept optional with the infrastructure designed to accommodate

ISBN: 978-3-95450-191-5 doi:10.18429/JACoW-SRF2017-THXA03

the extra cavities. The nominal voltage of 3.4 MV was chosen to operate the cavities well below the quench limit to minimize RF trips and ensure machine protection [2].

SPS BEAM TESTS

Beam tests of the compact crab cavities with hadron beams is considered as pre-requisite before an installation into the LHC [3]. The objective of these tests are four fold:

- Demonstration of cavity transparency when the cavities are not in use (for example during beam injection and energy ramp).
- Characterize failure scenarios and beam response during RF trips for machine protection.
- Demonstrate crabbing action and the entire RF sequence with high reliability and without degradation of the beam quality.
- Comprehensive beam measurements with protons such as crab optics, RF non-linearity, electrical center alignment, RF power including transients, beam stability, HOM power and other relevant aspects for system validation and stable operation.

A two-cavity test module is foreseen to be installed in the SPS during the upcoming technical shutdown of 2017-18. A mechanical bypass (see Fig. 3) is installed in the SPS BA6 region to allow for the cryomodule to be moved in and out only when required. Aperture restrictions for the filling of the LHC presently exclude the use of crab cavities in the SPS during regular operation [4].

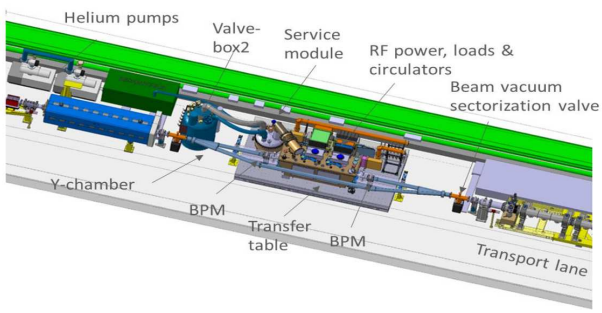

Figure 3: The SPS-BA6 region with a horizontal bypass for a crab cavity test module.

With the foreseen tests in 2018, the SPS-LLS6 region was modified with the new vacuum sectorization. The cryogenic and RF lines linking the surface equipment to the tunnel including majority of the cabling and handling equipment were installed in the 2016-17 shutdown [5]. The large equipment including the cryomodule, cold-box, mechanical bypass, movable table and all the surface powering equipment is expected to installed in the upcoming 2017-18 shutdown period.

CAVITY & CRYOMODULE STATUS

Very compact transverse size at 400 MHz are required to fit within LHC footprint while accommodating the long proton bunches. Two candidates fulfilling such criteria are under fabrication (see Fig. 4) for tests with proton beams in the SPS. Conventional elliptical cavities at this frequency is at least a factor of 4 larger than the available transverse separation between the beam chambers and would therefore be incompatible. In addition, the proposed compact cavity designs show superior RF properties compared to their elliptical counterparts [2, 6, 7].

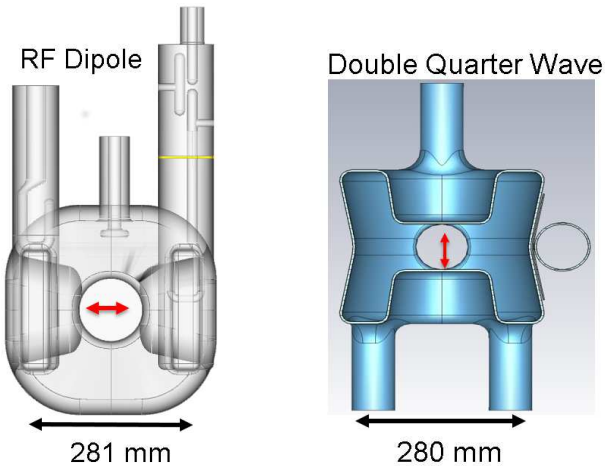

Figure 4: Two compact cavity designs considered for horizontal and vertical crabbing for the HL-LHC upgrade [2, 6, 7].

Table 2: Crab Cavity RF Parameters for HL-LHC. †The lower frequency is only required in the SPS to cover the energy range of 26-4500 GeV [4].

	Unit	HL-LHC
RF Frequency	[MHz]	$400.53^{\dagger}$ – 400.79
Cavity Aperture	[mm]	84
Design Voltage/Cavity	[MV]	3.4
Dynamic Losses	[W]	≤ 5.0
Tuning Range	[kHz]	±150
Lorentz Detuning	[Hz/MV^2]	≤ 865
dF/dp	[Hz/mbar]	≤ 150
Pole Symmetry	[mm]	≤ 0.7
Input Power, CW	[kW]	40
Input Coupler, Q_{ext}		5×10^5
Cavity filling time	[ms]	2.5
HOM Power/coupler	[kW]	1.0

Cavity Test Results

As a result of joint R&D between CERN, USLARP and the UK, a total of four DQW and two RFD cavities were fabricated in bulk Niobium as SPS prototypes. Each cavity was treated using the standard buffer chemical polishing, heat treatment & high pressure rinsing procedures adopted for SRF cavities. Four chemistry cycles and regulated etch rate were used on the CERN built DQW cavities to get a uniform removal of approximately 200 µm on the cavity [8].

ISBN: 978-3-95450-191-5 doi:10.18429/JACoW-SRF2017-THXA03

The performance of all cavities are well above the design target 3.4 MV with only a slightly higher surface resistance than the specified 10 nΩ. A summary of the test results with relevant parameters are listed in Table 3. Approximately 1 mR/h is assumed as the level for the onset of field emission (FE).

Dressed Cavities

Figure 5 shows a 3D section view of the different elements that make up the dressed cavity. The helium vessel serves a complex function of the cold mass enclosure and as the primary stiffening structure made of Ti with the added function frequency tuning interface [9]. This is particularly true for the DQW design and therefore designed to be structurally held by more than 250 Ti bolts with only superficial welds to ensure leak tightness. Ti grade 2 was chosen as the optimum material for the helium tank, allowing for rigid connection of cavity ports and minimize the stress on to the cavity during cool-down and other mechanical loading conditions [10]. An internal cold magnetic shield is used for additional magnetic field shielding due to the complex geometry and numerous interfaces of the cavity to the He-vessel. A symmetric tuning system to move the poles of the

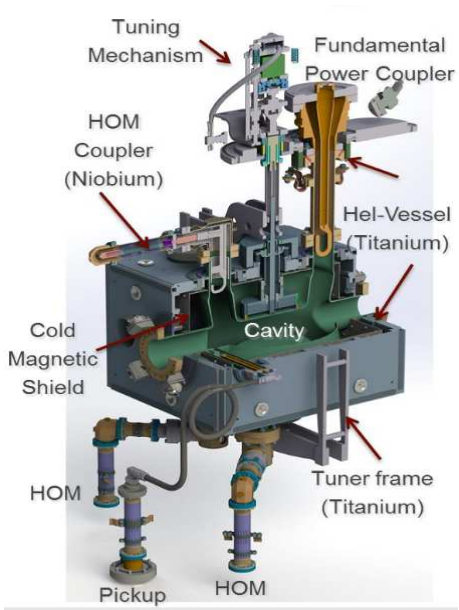

Figure 5: A 3D cross section of the DQW dressed cavity. The RFD dressed cavity differs mainly on the interfaces to the Helium vessel (courtesy CERN EN-MME).

DQW is adopted with differential movement of concentric Ti cylinders. In the RFD, the cavity body orthogonal to the poles are actuated to realize the symmetric tuning. The actuation is performed at warm outside of the cryostat. A three point support system using the double wall tube of the fundamental power coupler (FPC) and symmetric blades for precise positioning is used [11]. The engineering and assembly sequence of the He-tank are presented in Ref. [9].

There are three main RF interfaces, the FPC, HOMs and the pick up (PU). The FPC will use a single coaxial disk-type window to separate the cavity vacuum and the air side. The FPC is designed to handle up to 40 kW average power, although only ≤ 15-20 kW is required during stable operation due to negligible beam loading. A hook shape antenna specific to each cavity type is required as the coupling element to reach the $Q_e = 5\times10^5$ while minimizing the heating of the antenna from the fundamental mode field. Figure 7 shows a cross section of the DQW and RFD higher order mode (HOM) couplers respectively [6, 7]. Three HOM couplers on the DQW and two on the RFD are needed to reach the required damping within the HL-LHC impedance budget. A complex machining and assembly procedure was required to achieve the tight tolerances required for the strong HOM damping. Figure 8 shows one of the DQW HOM coupler to be used in the SPS cavities prior to its assembly.

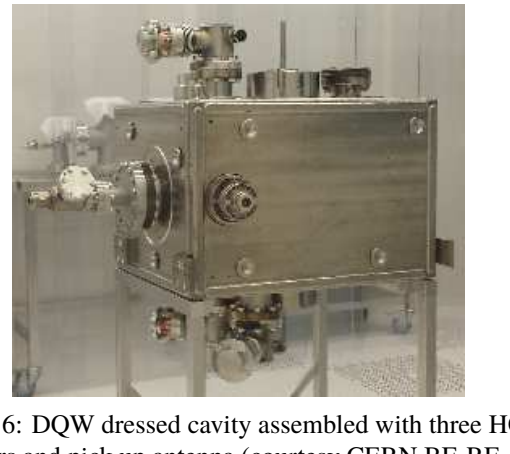

Figure 6: DQW dressed cavity assembled with three HOM couplers and pick up antenna (courtesy CERN BE-RF, EN-MME & TE-VSC).

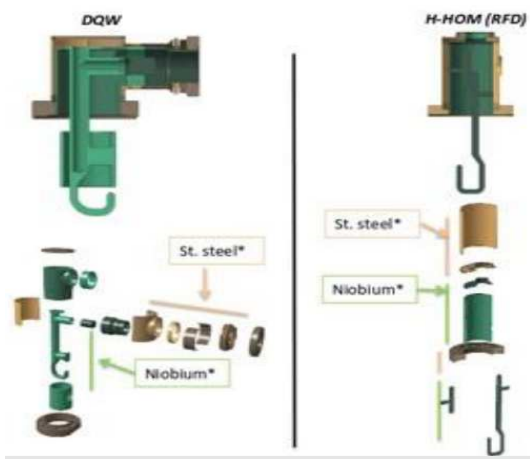

Figure 7: Top: HOM couplers for the DQW and the RFD cavities respectively using a 2-stage filter design (courtesy USLARP & CERN EN-MME).

Cryomodule

The cryomodules are designed to have a rectangular outer vacuum vessel with removable side panels such that the

ISBN: 978-3-95450-191-5 doi:10.18429/JACoW-SRF2017-THXA03

Table 3: Summary of the Cavity Cold Test Performance at CERN [12] and USLARP [13]. †Maximum voltage limited by RF power.

	Unit	DQW #1	DQW #2	DQW #1	DQW #2	RFD #1	RFD #2
		CERN		USLARP			
Max. Voltage	[MV]	5.04	4.8	5.8	5.3†	4.4	5.75
E_p, B_p	[MV/m, mT]	56, 109	54, 103	65, 125	59, 114	42, 73	56, 96
R_s	[nΩ]	10	10	9	9.5	11	7.6
R_s, 3.4 MV	[nΩ]	15	18	15	17	13	8.2
FE onset	[MV]	4.0	4.4	4.5	3.4	No FE	4.5

Figure 8: Bottom: DQW HOM coupler in bulk Nb with its stainless steel jacket for active cooling (courtesy CERN EN-MME).

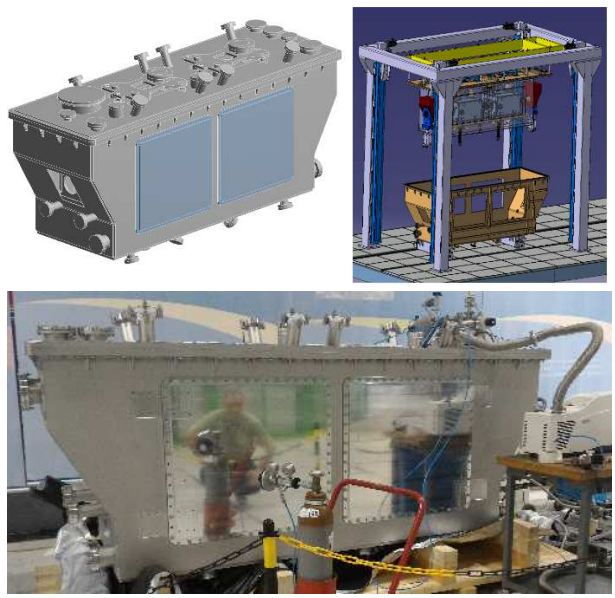

Figure 9: Top: The two-cavity cryomodule hosting the crab cavities (left) and the top loading assembly sequence (right). Bottom: Vacuum vessel under vacuum testing (courtesy CERN EN-MME).

dressed cavities remain accessible (see Fig. 9). Loading of the complete cavity string into the vacuum vessel is from the top, with plug valves fitted with closing end-plates integrated in the cavity string. All external connections except the beam pipes are on the top of the cryomodule. The cavities are supported by the outer tube of the power couplers. The vacuum vessel is fitted with stiffening ribs to keep the stress within reasonable limits when placed under vacuum pressure tests and during cool-down. The designs for both cavity variants are kept as similar as possible except for the RF interfaces specific to their design. The SPS DQW cryomodule mainly differs from the final LHC module due to the absence of the second beam pipe for the counter-rotating beam and additional vacuum interfaces for pumping.

RF SYSTEM

The overall architecture of the RF system and cavity powering in the LHC is shown in Fig. 10). The infrastructure is designed to accommodate the optional upgrade of doubling the crab cavity system to reach the full 12-13 MV required for the full compensation of the crossing angle. The high power RF services and the low level controls (LLRF) are placed in a common underground service gallery approximately 5 m above the LHC tunnel. This cavern allows access to the RF system while the LHC is operational. As shown in Fig. 10, the circulators are placed in an RF gallery directly above the LHC tunnel with 1 m diameter pits connecting the RF power waveguides to the cavities while the high power from the amplifiers to the circulators are through coaxial lines for a compact footprint.

Inductive Output Tubes (IOTs) are adopted as a baseline for the HL-LHC RF amplifiers given the adequate power overhead in a compact footprint. A 60 kW prototype at 400 MHz (see Fig. 11) was already qualified with two units under preparation for the SPS tests [14].

Each cavity is powered by its own RF amplifier for fast and independent control of voltage and phase to ensure precise control of the closed orbit and the crossing angle. Most importantly, the fast control of the cavity fields will minimize the risk to the LHC during an abrupt failure of one of the cavities, ensuring machine protection before the beams can be safely extracted. The strong local feedback on the deflecting mode is achieved with a short delay loop of ~2 µs [15]. A global loop regulating the vector sum of voltages on the two

ISBN: 978-3-95450-191-5 doi:10.18429/JACoW-SRF2017-THXA03

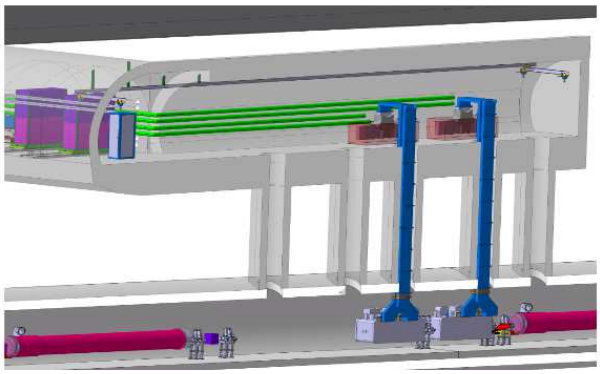

Figure 10: A sketch of the RF system and the crab cavity powering in the HL-LHC from the underground cavern above the LHC tunnel (Courtesy P. Fessia).

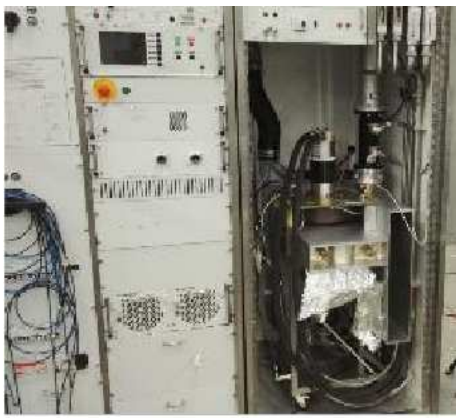

Figure 11: The SPS IOT system modified to 400 MHz and qualified to 60 kW (Courtesy E. Montesinos).

sides of the interaction region is also employed to account for drifts and slow transients.

Each two-cavity module will be equipped with a single PLC controller with a PLC cycle time estimated to be 2 ms and the fast interlock cycle time is 15 µs. The PLC will include the RF veto and vacuum signals, amplifier control, cavity tuning, high power interlocks, HOM interlocks, beam interlocks, cavity cryogenic interface and access in the RF zone [16].

CONCLUSIONS

The final design choices for the HL-LHC crab cavities in preparation for the SPS beam tests have been validated and robust. Several new and novel concepts were developed to adapt towards the crab cavity needs with adequate prototyping effort for each critical element. The lessons learned during the SPS test phase will be important element in finalizing the industrializing phase towards the HL-LHC fabrication.

ACKNOWLEDGMENTS

The author would like sincerely thank all the members of crab cavity collaboration and HL-LHC WP4 members for their valuable contributions and discussions. The authors would also like to extend a special thanks to BE-RF, EN-MME and TE-VSC groups at CERN for their invaluable contributions for this project.

REFERENCES

[1] HL-LHC Technical Design Report version 01, EDMS 1723851, 2017.

[2] R. Calaga, in *Proceedings of LHC Performance Workshop 2012*, Chamonix, France, 2012.

[3] S. Myers *et al.*, Summary of the 5^{th} Crab Cavity Workshop, LHC-CC11, CERN-ATS-2012-055, 2011.

[4] R. Calaga *et al.*, Summary of the SPS Test Day I, 2016.

[5] G. Vandoni *et al.*, presented at the International review of the Crab Cavity performance for HiLumi, CERN, 2017.

[6] S. De Silva *et al.*, "Design and Prototyping of a 400 MHz RF-dipole Crabbing Cavity for the LHC High-Luminosity Upgrade", in *Proc. IPAC'15*, Richmond, VA, USA, paper WEPWI036, 2015.

[7] S. Verdu *et al.*, "Design and Prototyping of HL-LHC Double Quarter Wave Crab Cavities for SPS Test", in *Proc. IPAC'15*, Richmond, VA, USA, paper MOBD2, 2015.

[8] T. Jones *et al.*, "Determining BCP Etch Rate and Uniformity in High Luminosity LHC Crab Cavities", presented at SRF2017, Lanzhou, China, paper TUPB100, 2017.

[9] M. Garlasche *et al.*, "Advanced Manufacturing Techniques for the Production of HL-LHC Crab Cavities at CERN", presented at SRF2017, Lanzhou, China, paper TUPB013, 2017.

[10] K. Artoos *et al.*, "Compact crab cavity cryomodule", CERN-ACC-2015-0130, 2015.

[11] T. Jones TUPB013, "Development of a Novel Supporting System for High Luminosity LHC SRF Crab Cavities", presented at SRF2017, Lanzhou, China, paper MOPB104, 2017.

[12] A. Castilla *et al.*, "First High-Q Validation of Crab Cavities for String Assembly at CERN", 2017.

[13] S. De Silva *et al.*, "RF Test of RF-Dipole Prototype Crabbing Cavity for LHC High Luminosity Upgrade", presented at SRF2017, Lanzhou, China, paper TUPB054, 2017.

[14] E. Montesinos, private communication.

[15] P. Baudrenghien, "LLRF for Crab Cavities", *2nd HiLumi LHC/LARP meeting*, Frascati, 2012.

[16] L. Arnaudon, private communication.